SixTrack Physics Manual (Draft)

R. De Maria, M. Fitterer, M. Fjellstrom, A. Patapenka

May 4, 2017

Contents

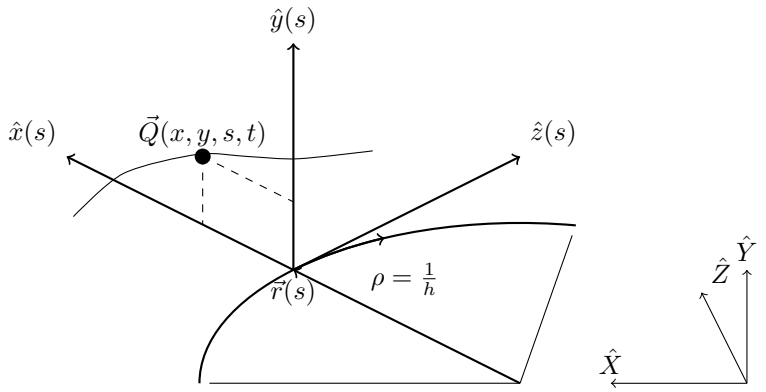

Figure 1: Moving reference frame $(\hat{x}, \hat{y}, \hat{z})$ parametrized by $s(t)$. The trajectory of a particle Q can be described by the coordinates (x, y, s, t).

1 Introduction

These notes give a short self-contained exposition of the physical assumptions and models implemented in SixTrack. Emphasis is given on the physical concepts rather then delving in to the details of the implementation. The content is meant to complement the SixTrack user guide (see [1]).

SixTrack is a 6D single particle symplectic tracking code used to compute the trajectories of individual relativistic charged particles in circular accelerators. It has been developed based on the 4D tracking code RaceTrack [2] by adding the third degree of freedom, introducing beam-beam forces and extending the pre- and post- processing capabilities.

The physical models are collected from the main references [3–9], which contain more details of the derivation of the maps.

2 Basic Principles and Hamiltonian formalism and notation

The speed, momentum, energy, rest mass, charge of a particle are indicated by v, P, E, m and q, respectively. These quantities are related by the following equations:

$$v = \beta c \qquad E^2 - P^2c^2 = m^2c^4 \qquad E = \gamma mc^2 \qquad Pc = \beta E \tag{1}$$

where β and γ are the relativistic factors.

In a curvilinear reference frame defined by a constant curvature h_x in the $\hat{X}, \hat{Z}$ plane and parameterized by s (see Fig. 1), the position of the particle at a time t can be written as:

$$\vec{Q}(t) = \vec{r}(s) + x\,\hat{x}(s) + y\,\hat{y}(s), \tag{2}$$

and therefore identified by the coordinates s, x, y, t in the reference frame defined by $\hat{x}(s)$ and $\hat{y}(s)$. In particle tracking, s is normally used as independent parameter and t as a coordinate.

The electromagnetic fields $\mathbf{E}$ and $\mathbf{B}$ can be derived in a curvilinear reference frame from the potentials $V(x, y, s, t)$ and $\mathbf{A}(x, y, s, t)$, where

$$\mathbf{A}(x, y, s, t) = A_x(x, y, s, t)\hat{x}(s) + A_y(x, y, s, t)\hat{y}(s) + A_s(x, y, s, t)\hat{z}(s) \tag{3}$$

and for which:

$$\mathbf{E} = -\nabla V - \frac{\partial \mathbf{A}}{\partial t} = -\partial_x V\hat{x} - \partial_y V\hat{y} - \frac{1}{1+hx}\partial_s V\hat{z} - \partial_t \mathbf{A} \tag{4}$$

$$\mathbf{B} = \nabla \times \mathbf{A} = \left(\partial_y A_s - \frac{\partial_s A_y}{1+hx}\right)\hat{x} + \cdots \tag{5}$$

$$\cdots + \left(\frac{\partial_s A_x}{1+hx} - \frac{hA_s}{1+hx} - \partial_x A_s\right)\hat{y} + (\partial_x A_y - \partial_y A_x)\,\hat{z}. \tag{6}$$

In this reference frame the canonical momenta are:

$$P_x = m\gamma\dot{x} + qA_x, \quad P_y = m\gamma\dot{y} + qA_y, \quad P_s = m\gamma\dot{s}(1+hx)^2 + q(1+hx)A_s. \tag{7}$$

If $s(t)$ is monotonically increasing, it is possible to derive the equations of motion using s as the independent parameter and t as a coordinate with $-E$ as the conjugate momentum. Since in accelerators the orbits of the particles are often a perturbation of the reference trajectory followed by a particle with rest mass m_0, charge q_0, speed $\beta_0 c$ and momentum P_0, one could use the following derived quantities that usually assume small values:

$$\Delta s = s - \beta ct \qquad c\Delta t = s/\beta_0 - ct \qquad \sigma = s - \beta_0 ct \tag{8}$$

$$\delta = \frac{P - P_0}{P_0} \qquad p_t = \frac{E - E_0}{P_0 c} \qquad p_\sigma = \frac{E - E_0}{\beta_0 P_0 c}. \tag{9}$$

and rescale the momenta according to:

$$p_x = P_x/P_0 \qquad p_y = P_y/P_0 \qquad p_s = P_s/P_0 \tag{10}$$

$$a_x = qA_x/P_0 \qquad a_y = qA_y/P_0 \qquad a_s = qA_s/P_0. \tag{11}$$

The corresponding Hamiltonians, kept implicit for brevity, are:

$$H\left(x, p_x, y, p_y, \sigma, p_\sigma; s\right) = p_\sigma - p_s \tag{12}$$

$$H\left(x, p_x, y, p_y, c\Delta t, p_t; s\right) = \frac{p_t}{\beta_0} - p_s \tag{13}$$

$$H\left(x, p_x, y, p_y, \Delta s, \delta; s\right) = \delta - p_s, \tag{14}$$

where

$$p_s = (1+hx)\left(\sqrt{(1+\delta)^2-(p_x-a_x)^2-(p_y-a_y)^2}+a_s\right) \tag{15}$$

$$\frac{P}{P_0} = 1+\delta = \sqrt{\left(\frac{E}{P_0 c}\right)^2-\left(\frac{mc}{P_0}\right)^2} = \sqrt{p_t^2+\frac{2p_t}{\beta_0}+\frac{1}{\beta_0^2}\left(1-\frac{m^2}{m_0^2}\right)+1} \tag{16}$$

$$\frac{E}{P_0 c} = \frac{1}{\beta_0}+p_t = \sqrt{\left(\frac{P}{P_0}\right)^2+\left(\frac{mc}{P_0}\right)^2} = \sqrt{(1+\delta)^2+\left(\frac{m}{m_0}\right)^2\left(\frac{1}{\beta_0\gamma_0}\right)^2} \tag{17}$$

$$(1+\delta)^2 = \beta_0^2 p_\sigma^2 + 2p_\sigma + 1 \qquad \beta = \frac{Pc}{E} = \frac{1+\delta}{1/\beta_0+p_t} \tag{18}$$

$$\tag{19}$$

In addition the following derivatives and approximations can be derived:

$$\delta \simeq p_\sigma - \frac{1}{\gamma_0^2}\cdot\frac{1}{2}p_\sigma^2 \qquad \frac{d\delta}{dp_\sigma} = \frac{\beta_0}{\beta} \simeq 1-\frac{p_\sigma}{\gamma_0^2} \qquad \frac{d^2\delta}{dp_\sigma^2} = -\frac{1}{\gamma_0^2}\cdot\left(\frac{p_0}{p}\right)^3 \tag{20}$$

$$\delta \simeq \frac{p_t}{\beta_0} - \frac{1}{\beta_0^2\gamma_0^2}\cdot\frac{1}{2}p_t^2 \quad \frac{d\delta}{dp_t} = \frac{1}{\beta} \simeq \frac{1}{\beta_0}-\frac{p_t}{\beta_0^2\gamma_0^2} \quad \frac{d^2\delta}{dp_t^2} = -\frac{1}{\beta_0^2\gamma_0^2}\cdot\left(\frac{p_0}{p}\right)^3 \tag{21}$$

3 Beam-line elements tracking maps

Each beam line elements is often characterized by a specific field configuration which determine the way the equation of motions are solved. The solutions of the equation of motion are typically explicit and derived by solving exactly the Hamilton equations for arbitrary initial conditions of an approximated Hamiltonian.

The following section illustrates the tracking maps used by SixTrack, labelled by the beam line elements that the maps approximately represent. The map is the solution of the equations of motion for a step L in the independent parameter s with a given set of initial conditions in the canonical coordinates. For brevity, when a coordinate is left unchanged by the map, the corresponding equation is omitted. High order integrators for single beam line elements can be built by combining simpler maps (e.g. thin kick and drifts).

The following maps use the canonical conjugate pairs (x, p_x), (y, p_y) and (σ, p_σ). It should be noted that SixTrack compute x' and y' during tracking instead of the momentum coordinates p_x and p_y and (E, E_0), (P, P_0) instead of p_σ. The canonical variables are used instead for the generation of linear and higher order symplectic maps needed for action-angle variable transformations and Twiss parameter extraction.

3.1 Drift

A drift is a straight, field-free region ($h_{x,y} = 0$, $V = 0$ and $\mathbf{A} = 0$). The exact and expanded Hamiltonian for a drift space are

$$H = p_\sigma - \sqrt{(1+\delta)^2 - p_x^2 - p_y^2} \approx p_\sigma - \delta + \frac{1}{2}\frac{p_x^2 + p_y^2}{1+\delta}. \tag{22}$$

With the help of the following definitions:

$$x_p = \frac{P_x}{P_0(1+\delta)} \simeq \frac{p_x}{p_z} = x', \qquad y_p = \frac{P_y}{P_0(1+\delta)} \simeq \frac{p_y}{p_z} = y', \tag{23}$$

the map relative to the expanded Hamiltonian is (eq. 3.49 in [5])

$$x \to x + x_p L \qquad y \to y + y_p L \tag{24}$$

$$c\Delta t \to c\Delta t + \frac{L}{\beta_0} - \frac{L}{\beta}\left(1 + \frac{x_p^2 + y_p^2}{2}\right) \qquad \Delta s \to \Delta s - \frac{x_p^2 + y_p^2}{2} \tag{25}$$

$$\sigma \to \sigma + L - \beta_0 \frac{L}{\beta}\left(1 + \frac{x_p^2 + y_p^2}{2}\right). \tag{26}$$

With the additional definitions:

$$p_z = \frac{P_z}{P_0} \tag{27}$$

$$p_z = \sqrt{(1+\delta)^2 - p_x^2 - p_y^2} = \sqrt{\beta_0^2 p_\sigma^2 + 2p_\sigma + 1 - p_x^2 - p_y^2}, \tag{28}$$

$$\beta_z = \beta\frac{P_z}{P} = \frac{p_z}{1+\delta} = \frac{p_z}{1/\beta_0 + p_t} = \frac{p_z}{1/\beta_0 + \beta_0 p_\sigma}, \tag{29}$$

the map of the exact Hamiltonian (eq. A.6a in [6]) is

$$x \to x + x' L \qquad y \to y + y' L \tag{30}$$

$$c\Delta t \to c\Delta t + \left(\frac{1}{\beta_0} - \frac{1}{\beta_z}\right) \cdot L \qquad \Delta s \to \Delta s + \frac{p_z - 1 - \delta}{p_z} \cdot L \tag{31}$$

$$\sigma \to \sigma + \left(1 - \frac{\beta_0}{\beta_z}\right) \cdot L \qquad \sigma \to \sigma + \frac{p_z - 1 - \beta_0^2 p_\sigma}{p_z} \cdot L. \tag{32}$$

It is possible to define a "polar" drift that has the effect of rotating the reference frame [10] for instance in the x-z plane:

$$p_x \to p_x \cos\theta + p_z \sin\theta \qquad p_z \to -p_x \sin\theta + p_z \cos\theta \tag{33}$$

$$z = -x \sin\theta \qquad x' = p_x/p_z \qquad y' = p_y/p_z \tag{34}$$

$$x \to x\cos\theta - x' z \qquad y \to y - x' z \tag{35}$$

$$\Delta s \to \Delta s + \frac{1+\delta}{p_z} z \qquad \sigma \to \sigma + \frac{\beta_0}{\beta_z} z. \tag{36}$$

where θ is the angle bringing the new $\hat{x}$ towards the old $\hat{z}$. The map can be also generated by combining a rotation with a $-x\sin(\theta)$-length drift. This map is not used in SixTrack.

3.2 Dipole

In a curvilinear reference system with a constant curvature h_x in the horizontal plane or h_y in the vertical plane (but not both, i.e. $h_x \cdot h_y = 0$) a uniform magnetic field can be derived by the vector potential:

$$A_x = 0, \qquad A_y = 0, \qquad A_s = -B_y x \left(1 - \frac{h_x x}{2(1+h_x x)}\right), \tag{37}$$

where we have chosen $h_y = 0$. Often the bending radius of the dipole correspond to $h_{x,y} = \frac{q_0}{p} B_{x,y}$, where q_0 is the charge of the reference particle, which simplify the Hamiltonian further. In these conditions the exact and expanded Hamiltonian for a horizontal bending magnet is (eq. 2.12 in [4])

$$H = p_\sigma - p_s + q \cdot h_x x \left(1 + \frac{h_x x}{2}\right) \tag{38}$$

$$\approx p_\sigma + \frac{1}{2}\frac{p_x^2 + p_y^2}{1+\delta} - h_x x(1+\delta) + \frac{q}{q_0} h_x x \left(1 + \frac{h_x x}{2}\right) \tag{39}$$

3.2.1 Thick dipole

Defining the following quantities,

$$G_x = \frac{q}{q_0} \cdot \frac{h_x^2}{1+\delta}, \qquad G_y = \frac{q}{q_0} \cdot \frac{h_y^2}{1+\delta} \tag{40}$$

$$C_{x,y} = \cos(\sqrt{G_{x,y}} L), \qquad S_{x,y} = \sin(\sqrt{G_{x,y}} L) \tag{41}$$

the map relative to the expanded Hamiltonian is (eq. 4.11 in [4])

$$\begin{aligned}
x &\to C_x \cdot x + \frac{S_x}{\sqrt{G_x}} \frac{1}{1+\delta} \cdot p_x + \frac{\delta}{h_x}(1 - C_x) \\
p_x &\to -\sqrt{G_x}(1+\delta) \cdot S_x \cdot x + C_x \cdot p_x + \delta\sqrt{1+\delta} \cdot S_x \\
y &\to C_y \cdot y + \frac{S_y}{\sqrt{G_y}} \frac{1}{1+\delta} \cdot p_y + \frac{\delta}{h_y}(1 - C_y) \\
p_y &\to -\sqrt{G_y}(1+\delta) \cdot S_y \cdot y + C_y \cdot p_y + \delta\sqrt{1+\delta} \cdot S_y \\
\sigma &\to \sigma + L\left(1 - \frac{\beta_0}{\beta}\right) \\
&\quad - \frac{\beta_0}{\beta}\left[\frac{h_x S_x}{\sqrt{G_x}} \cdot x + \frac{1 - C_x}{h_x} \cdot p_x + \frac{h_y S_y}{\sqrt{G_y}} \cdot y + \frac{1 - C_y}{h_y} \cdot p_y + \delta\left(2L - \frac{S_x}{\sqrt{G_x}} - \frac{S_y}{\sqrt{G_y}}\right)\right] \\
&\quad - \frac{1}{4}\frac{\beta_0}{\beta}\left[G_x\left(L - \frac{C_x S_x}{\sqrt{G_x}}\right)\left(x - \frac{\delta}{h_x}\right)^2 + \left(L + \frac{C_x S_x}{\sqrt{G_x}}\right)\frac{p_x^2}{(1+\delta)^2} - \left(x - \frac{\delta}{h_x}\right)\frac{2S_x^2}{1+\delta} \cdot p_x\right. \\
&\quad \left. + G_y\left(L - \frac{C_y S_y}{\sqrt{G_y}}\right)\left(y - \frac{\delta}{h_y}\right)^2 + \left(L + \frac{C_y S_y}{\sqrt{G_y}}\right)\frac{p_y^2}{(1+\delta)^2} - \left(y - \frac{\delta}{h_y}\right)\frac{2S_y^2}{1+\delta} \cdot p_y\right].
\end{aligned}$$

An alternative version of the ideal sector bend (eq. 12.18 in [10]) with arbitrary bending field $b_1 = \frac{q_0}{P_O} B_y$ and reference radius ρ is

$$\alpha(s) = \sin^{-1}\left(\frac{p_x(s)}{\sqrt{(1+\delta^2) - p_y^2}}\right) \tag{42}$$

$$p_z(s) = \sqrt{(1+\delta)^2 - p_x^2(s) - p_y^2} \tag{43}$$

$$x \to \frac{\rho}{b_1}\left(\frac{1}{\rho}p_z(L) - p_x'(L) - b_1\right) \tag{44}$$

$$p_x \to p_x \cos(\theta) + (p_z(0) - b_1(\rho + x))\sin(\theta) \tag{45}$$

$$y \to y + \frac{p_y L}{b_1 \rho} + \frac{p_y}{b_1}(\alpha(0) - \alpha(L)) \tag{46}$$

$$ct \to ct + \frac{(1+\delta)L}{b_1\rho} + \frac{(1+\delta)}{b_1}(\alpha(0) - \alpha(L)) \tag{47}$$

where $\theta = hL$ is the bending angle. This map is numerically unstable for $L \to 0$, $b_1 \to 0$, $\rho \to \infty$. This map is not used in SixTrack.

3.2.2 Thin dipole

The map for a thin dipole kick (horizontal or vertical) from the expanded Hamiltonian is (eq. 4.12 in [6]):

$$p_x \to p_x - \frac{q}{q_0} \cdot (h_x L)(1 + h_x x) + (h_x L)(1+\delta) \tag{48}$$

$$p_y \to p_y - \frac{q}{q_0} \cdot (h_y L)(1 + h_y y) + (h_y L)(1+\delta) \tag{49}$$

$$\sigma \to \sigma - \frac{\beta_0}{\beta}(h_x x + h_y y)L. \tag{50}$$

The map for a horizontal ($h_y = 0$) thin dipole with the exact Hamiltonian can be expressed as (eq. 3.21 in [7]) $T_{II}(L/2) \circ T_I(L) \circ T_{II}(L/2)$ where $T_{II}(L)$ is given by

$$p_x \to \frac{1}{1 + (h_x L)^2}\left[p_x + (h_x L)(1+\delta)\left(\sqrt{1 - \frac{p_x^2 + p_y^2 - C}{(1+\delta)^2}} - 1\right)\right] \tag{51}$$

$$x \to x + (h_x L) \cdot x \cdot \frac{p_x}{p_z} \tag{52}$$

$$y \to y + (h_x L) \cdot x \cdot \frac{p_y}{p_z} \tag{53}$$

$$\sigma \to \sigma + (h_x L) \cdot x \cdot \left(\frac{\beta_0}{\beta} - \frac{\beta_0}{\beta_z}\right), \tag{54}$$

with $C = -(h_x L)^2 p_y^2 + 2(h_x L)(1+\delta)p_x$ and $T_I(L)$ is given by

$$p_x \to p_x - h_x^2 L x + (h_x L) \cdot \delta \tag{55}$$

$$\sigma \to \sigma - (h_x L) x \cdot \frac{\beta_0}{\beta}. \tag{56}$$

In order to represent a dipole of length L this map is to be combined with two surrounding drift spaces using the exact Hamiltonian, each of half the length of the dipole.

The exact thin dipole could be also generated by the composition of

$$D(-L/2) \circ D_p(\theta/2) \circ K(L) \circ D_p(\theta/2) \circ D(L/2) \tag{57}$$

for which D is a drift, D_p a polar drift and K the map generated by $K = b_y(x + \frac{h_x}{2}x^2)$. This map is not used in SixTrack.

3.2.3 Dipole Edge effects

The dipole edge effects from a dipole of length L and bending angle θ can be approximated by the map:

$$p_x \to p_x + \frac{1+\delta}{\rho} \tan(\alpha) \cdot x \tag{58}$$

$$p_y \to p_y - \frac{1+\delta}{\rho} \tan(\alpha) \cdot y, \tag{59}$$

where the bending radius ρ and α are defined as

$$\rho^{-1} = \frac{h_x}{\sqrt{1+\delta}} \qquad\qquad \alpha = \frac{1}{2}\frac{L}{\rho} = \frac{\theta}{2}. \tag{60}$$

.

3.3 Quadrupole

A quadrupole is characterized by the vector potential

$$a_x = 0 \qquad a_y = 0 \qquad a_s = -\frac{1}{2}k_1(y^2 - x^2). \tag{61}$$

The expanded Hamiltonian for a particle in a quadrupole is

$$H = p_\sigma - \delta + \frac{1}{2}\frac{p_x^2 + p_y^2}{1+\delta} + \frac{1}{2}k_1(x^2 - y^2). \tag{62}$$

3.3.1 Thick quadrupole

By defining the following quantities

$$g = q \cdot \frac{g_0}{1+\delta} \tag{63}$$

we have the following two cases

$$C = \begin{cases} \cos(\sqrt{g}L) & g > 0 \\ \cosh(\sqrt{-g}L) & g < 0 \end{cases} \qquad S = \begin{cases} \sin(\sqrt{g}L) & g > 0 \\ \sinh(\sqrt{-g}L) & g < 0 \end{cases} \tag{64}$$

$$\hat{C} = \begin{cases} \cosh(\sqrt{-g}L) & g > 0 \\ \cos(\sqrt{g}L) & g < 0 \end{cases} \qquad \hat{S} = \begin{cases} \sinh(\sqrt{-g}L) & g > 0 \\ \sin(\sqrt{g}L) & g < 0 \end{cases} \tag{65}$$

Using the above definitions the map of a thick quadrupole is (eq. 4.2 in [4])

$$x \to C \cdot x + \frac{S}{\sqrt{|g|}} \frac{p_x}{1+\delta} \tag{66}$$

$$p_x \to -(1+\delta)\sqrt{|g|} S \cdot x + C \cdot p_x \tag{67}$$

$$y \to \hat{C} \cdot y + \frac{\hat{S}}{\sqrt{|g|}} \frac{p_y}{1+\delta} \tag{68}$$

$$p_y \to (1+\delta)\sqrt{|g|} \hat{S} \cdot y + \hat{C} \cdot p_y \tag{69}$$

$$\sigma \to \sigma + L\left(1 - \frac{\beta_0}{\beta}\right) - \frac{|g|}{4}\frac{\beta_0}{\beta}\left[\left(L - \frac{C \cdot S}{\sqrt{|g|}}\right) \cdot x^2 - \left(L - \frac{\hat{C} \cdot \hat{S}}{\sqrt{|g|}}\right) \cdot y^2\right] \tag{70}$$

$$- \frac{1}{4}\frac{\beta_0}{\beta}\left[\left(L + \frac{C \cdot S}{\sqrt{|g|}}\right) \cdot \frac{p_x^2}{(1+\delta)^2} + \left(L + \frac{\hat{C} \cdot \hat{S}}{\sqrt{|g|}}\right) \frac{p_y^2}{(1+\delta)^2}\right] \tag{71}$$

$$- \frac{1}{2}\frac{\beta_0}{\beta}\left[- x \cdot \frac{p_x}{1+\delta} \cdot S^2 + y \cdot \frac{p_y}{1+\delta} \hat{S}^2\right]. \tag{72}$$

3.3.2 Thick skew quadrupole

The Hamiltonian for a skew quadrupole

$$H = p_\sigma - \delta + \frac{1}{2}\frac{p_x^2 + p_y^2}{1+\delta} - N \cdot xy, \tag{73}$$

where $N = \frac{1}{2}\frac{q}{E_0}\left(\frac{\partial B_x}{\partial x} - \frac{\partial B_y}{\partial y}\right)_{x=y=0}$. For a thick skew quadrupole the map is (eq. 3.19, 3.20 in [3])

$$x \to C^+ \cdot x + S^+ \cdot p_x - C^- \cdot y - S^- \cdot p_y \tag{74}$$

$$p_x \to -\hat{S}^- \cdot x + C^+ \cdot p_x + \hat{S}^+ \cdot y - C^- \cdot p_y \tag{75}$$

$$y \to -C^- \cdot x - S^- \cdot p_x + C^+ \cdot y + S^+ \cdot p_y \tag{76}$$

$$p_y \to \hat{S}^+ \cdot x - C^- \cdot p_x - \hat{S}^- \cdot y + C^+ \cdot p_y \tag{77}$$

$$\sigma \to \sigma + \frac{1}{8}(x^2 + y^2)\left(C^+\hat{S}^- + C^-\hat{S}^+\right) \tag{78}$$

$$- \frac{1}{8}\frac{p_x^2 + p_y^2}{(1+\delta)^2}\left[L + C^+S^+ + C^-S^-\right] \tag{79}$$

$$+ \frac{1}{2}Nxy\left[L - C^+S^+ - C^-S^-\right] + \frac{1}{2}\frac{p_x p_y}{(1+\delta)^2}\left[C^+S^- + C^-C^+\right] \tag{80}$$

$$+ \frac{xp_x + yp_y}{1+\delta}S^+\hat{S}^- - \frac{xp_y + p_x y}{1+\delta}\frac{1}{2}\left[S^+\hat{S}^- + S^-\hat{S}^+\right] \tag{81}$$

where

$$C^- = \frac{\cos\sqrt{N}L - \cosh\sqrt{N}L}{2} \qquad C^+ = \frac{\cos\sqrt{N}L + \cosh\sqrt{N}L}{2} \tag{82}$$

$$S^- = \frac{\sin\sqrt{N}L - \sinh\sqrt{N}L}{2\sqrt{N}} \qquad S^+ = \frac{\sin\sqrt{N}L + \sinh\sqrt{N}L}{2\sqrt{N}} \tag{83}$$

$$\hat{S}^- = \frac{\sqrt{N}}{2}(\sin\sqrt{N}L - \sinh\sqrt{N}L) \quad \hat{S}^+ = \frac{\sqrt{N}}{2}(\sin\sqrt{N}L + \sinh\sqrt{N}L) \tag{84}$$

3.4 Combined function magnet

3.4.1 Thin combined function magnet

The map is the combination of the map for the thin dipole and for a thin quadrupole using the thin multipole expansion (eq. 3.12 in [5])

$$p_x \to p_x - G_1 L \cdot x + (1+\delta)h_x L - q \cdot h_x L \tag{85}$$

$$p_y \to p_y - G_2 L \cdot y + (1+\delta)h_y L - q \cdot h_y L \tag{86}$$

$$\sigma \to \sigma - \frac{\beta_0}{\beta}(h_x x + h_y y)L, \tag{87}$$

where $G_1 = q \cdot h_x^2 + k_1$ and $G_2 = q \cdot h_y^2 - k_1$.

3.5 Thin Multipole

A longitudinally uniform static magnetic field can be described by the following equations

$$A_z = -\Re \sum_{n=1} \frac{1}{n} \left(B_n + iA_n\right) \frac{(x+iy)^n}{r_0^{n-1}} \tag{88}$$

$$B_y + iB_x = \sum_{n=1} \left(B_n + iA_n\right) \frac{(x+iy)^{n-1}}{r_0^{n-1}}. \tag{89}$$

A thin multiple idealize the effect of the field by taking the limit of the integration length going to zero while keeping constant the integrated strength. The Hamiltonian is:

$$H = -\delta(s) L \frac{q}{p} A_z. \tag{90}$$

The corresponding map is:

$$p_x \to p_x - L \cdot \Re \left[\sum_{n=0} \frac{1}{n!} (k_n + i\hat{k}_n)(x+iy)^n \right], \tag{91}$$

$$p_y \to p_y + L \cdot \Im \left[\sum_{n=0} \frac{1}{n!} (k_n + i\hat{k}_n)(x+iy)^n \right], \tag{92}$$

for which

$$k_n = \frac{q}{p} \frac{\partial^n B_y}{\partial x^n} = \frac{q}{p} \frac{n!}{r_0^n} B_{n+1} \qquad B_{n+1} = \frac{r_0^n}{n!} \frac{\partial^n B_y}{\partial x^n} \tag{93}$$

$$\hat{k}_n = \frac{q}{p} \frac{\partial^n B_x}{\partial x^n} = \frac{q}{p} \frac{n!}{r_0^n} A_{n+1} \qquad A_{n+1} = \frac{r_0^n}{n!} \frac{\partial^n B_x}{\partial x^n} \tag{94}$$

For instance, the map for a normal quadrupole, sextupole and octupole are :

$$p_x \to p_x - L \cdot k_1 \cdot x \qquad p_y \to p_y + L \cdot k_1 \cdot y, \tag{95}$$

$$p_x \to p_x - L \cdot \frac{k_2}{2} \cdot (x^2 - y^2) \qquad p_y \to p_y + L \cdot k_2 \cdot xy, \tag{96}$$

$$p_x \to p_x - L \cdot \frac{k_3}{6} \cdot (x^3 - 3xy^2) \qquad p_y \to p_y + L \cdot \frac{k_3}{6} \cdot (3x^2 y - y^3). \tag{97}$$

3.6 RF-cavity

The expanded Hamiltonian for a RF-cavity is (eq. 2.30 in [5])

$$H = p_\sigma + \frac{1}{\beta_0^2} \frac{C}{2\pi h_a} \frac{qV(s)}{E_0} \cos\left(h_a \frac{2\pi}{C} \sigma + \varphi \right), \tag{98}$$

where h_a is the harmonic number, φ is the phase angle, V is the voltage and C is the design circumference length. The thin lens transfer map is (eq. 3.44 in [5])

$$p_\sigma \to p_\sigma + \frac{1}{\beta_0^2}\frac{qV(s_0)}{E_0}\cdot\sin\left(h_a\frac{2\pi}{C}\sigma+\varphi\right). \tag{99}$$

Using the relation between p_σ and the energy E, the map can be expressed as the change in energy of the tracked particle

$$E \to E + q\cdot V\sin\left(h_a\frac{2\pi}{C}\sigma+\varphi\right). \tag{100}$$

This is how Sixtrack performs the calculation.

3.7 Solenoid

The expanded Hamiltonian for a particle in a solenoid is

$$H = p_\sigma + \frac{1}{2}\frac{(p_x+R\cdot y)^2+(p_y-R\cdot x)}{1+\delta}, \tag{101}$$

where $R=\frac{1}{2}\frac{q}{P_0c}\mathbf{B}(0,0,s)$. The map for a solenoid of length L in the thin lens approximation with the expanded Hamiltonian (eq. 4.35 in [6])

$$\begin{aligned}
x &\to \quad C\cdot x + S\cdot y && (102)\\
p_x &\to -\theta R\cdot C\cdot x + C\cdot p_x - \theta R\cdot S\cdot y + S\cdot p_y && (103)\\
y &\to -S\cdot x + C\cdot y && (104)\\
p_y &\to \quad \theta R\cdot S\cdot x - S\cdot p_x - \theta R\cdot C\cdot y + C\cdot p_y && (105)\\
\sigma &\to \sigma - \frac{\beta_0}{\beta}\frac{\theta}{1+\delta}\left(\frac{1}{2}R(x^2+y^2)+(p_xy-p_yx)\right) && (106)
\end{aligned}$$

where $R\equiv R(s_0)$, $\theta=\frac{R}{1+\delta}$, $C=\cos(\theta)$ and $S=\sin(\theta)$.

The map for a thick solenoid is (eq. 3.47, 3.48 in [3])

$$\begin{aligned}
x &\to C^2\cdot x + \frac{1}{R}\cdot S\cdot C\cdot p_x + S\cdot C\cdot y + \frac{1}{R}\cdot S^2\cdot p_y && (107)\\
p_x &\to -R\cdot S\cdot C\cdot x + C^2\cdot p_x - R\cdot S^2\cdot y + S\cdot C\cdot p_y && (108)\\
y &\to -S\cdot C\cdot x - \frac{1}{R}\cdot S^2\cdot p_x + C^2\cdot y + \frac{1}{R}\cdot S\cdot C\cdot p_y && (109)\\
p_y &\to R\cdot S^2\cdot x - S\cdot C\cdot p_x - R\cdot S\cdot C\cdot y + C^2\cdot p_y && (110)\\
\sigma &\to \sigma - \frac{L}{2}\left[R^2(x^2+y^2)+2R\left(\frac{p_x}{1+\delta}y-\frac{p_y}{1+\delta}x\right)+\frac{p_x^2+p_y^2}{(1+\delta)^2}\right] && (111)
\end{aligned}$$

where $\theta = R\cdot L$, $C=\cos\theta$ and $S=\sin\theta$.

3.8 Beam-beam lens

In order to study beam-beam interactions the strong bunch can be split longitudinally into several slices, each slice described by an electrostatic potential of the form (eq. 2.1 in [8])

$$\hat{U}(x,y;\hat{\Sigma}_{11},\hat{\Sigma}_{33};\theta) \equiv U(\hat{x},\hat{y};\hat{\Sigma}_{11},\hat{\Sigma}_{33}) = -\frac{r_p}{\gamma_0}\int_0^\infty \frac{\exp\left(-\frac{\hat{x}^2}{2\hat{\Sigma}_{11}+u}-\frac{\hat{y}^2}{2\hat{\Sigma}_{33}+u}\right)}{\sqrt{2\hat{\Sigma}_{11}+u}\sqrt{2\hat{\Sigma}_{33}+u}}du, \tag{112}$$

where Σ_{ij} are the elements of the 6×6 phase-space envelope matrix of the strong bunch.

To evaluate the effect of the beam-beam interaction on a test particle two sets of transformations need to be considered. The first is a transformation of Cartesian to accelerator coordinates and a Lorentz boost making the collision between the bunches head-on, this is accomplished by the Lorentz transformation given by (eq. 2.21 in [8])

$$\mathcal{L} = \begin{pmatrix} \frac{1}{\cos\phi} & -\cos\alpha\sin\phi & -\tan\phi\sin\phi & -\sin\alpha\sin\phi \\ -\cos\alpha\tan\phi & 1 & \cos\alpha\tan\phi & 0 \\ 0 & -\cos\alpha\sin\phi & \cos\phi & -\sin\alpha\sin\phi \\ -\sin\alpha\tan\phi & 0 & \sin\alpha\tan\phi & 1 \end{pmatrix}, \tag{113}$$

where α is the crossing plane angle and 2ϕ is the total crossing angle. The second set of transformations is called the Synchro-Beam Mapping (SBM). In the SBM the test particle at the interaction point (IP) is brought to the collision point by a drift, then the beam-beam interaction is applied and finally the position of the test particle is brought back to the IP.

For a test particle with Lorentz transformed coordinates $(x^*,p_x^*,y^*,p_y^*,z^*,p_z^*)$ the explicit form for the SBM is (eq. 2.65 in [8])

$$x^* \to x^* + Sn^*F_x^* \tag{114}$$

$$p_x^* \to p_x^* - n^*F_x^* \tag{115}$$

$$y^* \to y^* + Sn^*F_y^* \tag{116}$$

$$p_y^* \to p_y^* - n^*F_y^* \tag{117}$$

$$p_z^* \to p_z^* - n^*F_z^* - \frac{1}{2}\left[n^*F_x^*(p_x^* - \frac{1}{2}n^*F_x^*) + n^*F_y^*(p_y^* - \frac{1}{2}n^*F_y^*)\right], \tag{118}$$

where n^* is the number of particles in the slice S is the distance between a test particle and the strong bunch and

$$F_x^* = \frac{\partial}{\partial\bar{x}^*}\hat{U}(\bar{x}^*,\bar{y}^*;\hat{\Sigma}_{11}(\varphi),\hat{\Sigma}_{33}(\varphi);\theta(\varphi)) \tag{119}$$

$$F_y^* = \frac{\partial}{\partial\bar{y}^*}\hat{U}(\bar{x}^*,\bar{y}^*;\hat{\Sigma}_{11}(\varphi),\hat{\Sigma}_{33}(\varphi);\theta(\varphi)) \tag{120}$$

$$F_z^* = \frac{\partial}{\partial\bar{z}^*}\hat{U}(\bar{x}^*,\bar{y}^*;\hat{\Sigma}_{11}(\varphi),\hat{\Sigma}_{33}(\varphi);\theta(\varphi)), \tag{121}$$

which are calculated from the expression for $\hat{U}$ given above. Finally the inverse Lorentz transformation $\mathcal{L}^{-1}$ is applied to the SBM transformed coordinates.

3.9 Beam-beam element

In the following, r_e is the classical electron radius and S is the strength ratio with respect to the nominal beam-beam kick strength. The maps below assumes no linear coupling between the transverse planes.

3.9.1 Round beam

Definitions

$$r_x = x - x_{\text{co}} + x_{\text{sep}}, \tag{122}$$
$$r_y = y - y_{\text{co}} + y_{\text{sep}}, \tag{123}$$
$$r^2 = r_x^2 + r_y^2. \tag{124}$$

The kick is

$$p_x \to p_x + r_e \cdot S \cdot \frac{r_x}{r^2}\left[1 - \exp\left(\frac{r^2}{2\sigma^2}\right)\right] - \text{beamoff}(4), \tag{125}$$
$$p_y \to p_y + r_e \cdot S \cdot \frac{r_y}{r^2}\left[1 - \exp\left(\frac{r^2}{2\sigma^2}\right)\right] - \text{beamoff}(5). \tag{126}$$

3.9.2 Elliptical beam

For this map, it is assumed that $x > y$ (i.e. the horizontal extension of the beam is larger than the vertical extension.) For the reverse case, $y > x$, interchange x and y in the map.

$$r_x = x - x_{\text{co}} + x_{\text{sep}}, \tag{127}$$
$$r_y = y - y_{\text{co}} + y_{\text{sep}}, \tag{128}$$
$$\bar{\sigma} = \sqrt{2(\sigma_x^2 - \sigma_y^2)}. \tag{129}$$

The kick is

$$p_x \to p_x + \text{sgn}(r_x)\left[r_e \cdot S\frac{\sqrt{\pi}}{\bar{\sigma}}\left(\text{erf}\left(\frac{|r_y|}{\bar{\sigma}}\right) - \exp\left(-\frac{1}{2}\left[\frac{r_x^2}{\sigma_x^2} + \frac{r_y^2}{\sigma_y^2}\right]\right)\text{erf}\left(\frac{\sigma_x}{\sigma_y}\frac{|r_y|}{\bar{\sigma}}\right)\right)\right] - \text{beamoff}(4), \tag{130}$$

$$p_y \to p_y + \text{sgn}(r_y)\left[r_e \cdot S\frac{\sqrt{\pi}}{\bar{\sigma}}\left(\text{erf}\left(\frac{|r_x|}{\bar{\sigma}}\right) - \exp\left(-\frac{1}{2}\left[\frac{r_x^2}{\sigma_x^2} + \frac{r_y^2}{\sigma_y^2}\right]\right)\text{erf}\left(\frac{\sigma_y}{\sigma_x}\frac{|r_x|}{\bar{\sigma}}\right)\right)\right] - \text{beamoff}(5). \tag{131}$$

3.10 Hirata's beam-beam element

Initial transformation of coordinates.

$$x_i \to (x + dx) - x_{\rm co} \tag{132}$$
$$p_{x,i} \to p_x - p_{x,\rm co} \tag{133}$$
$$y_i \to (y + dy) - y_{\rm co} \tag{134}$$
$$p_{y,i} \to p_y - p_{y,\rm co} \tag{135}$$
$$\sigma_i \to \sigma - \sigma_{\rm co} \tag{136}$$
$$\delta_i \to \delta - \delta_{\rm co}. \tag{137}$$

Lorentz boost. ϕ is the crossing plane angle and α is the half crossing angle. The particle has initial coordinates $(x^i, p_x^i, y^i, p_y^i, \sigma^i, \delta^i)$. We define $h = (1+\delta^i) - \sqrt{(1+\delta^i)^2 - (p_x^i)^2 - (p_y^i)^2}$. p_z is computed with the most recent values of δ, p_x and p_y.

$$\delta \to \delta^i - \cos\alpha\tan\phi\cdot p_x^i - \sin\alpha\tan\phi\cdot p_y^i + h\cdot\tan^2\phi \tag{138}$$
$$p_x \to p_x^i\frac{1}{\cos\phi}\left(p_x^i - \tan\phi\cos\alpha\cdot h\right) \tag{139}$$
$$p_y \to p_y^i\frac{1}{\cos\phi}\left(p_y^i - \tan\phi\sin\alpha\cdot h\right) \tag{140}$$
$$\sigma \to \frac{\sigma^i}{\cos\phi} + \left(1 - \frac{1+\delta}{p_z}\right)\left(\sin\phi\cos\alpha\cdot x^i + \sin\phi\sin\alpha\cdot y^i\right) \tag{141}$$
$$x \to \cos\alpha\tan\phi\cdot\sigma + \left(1 + \cos\alpha\sin\phi\frac{p_x}{p_z}\right)\cdot x^i + \sin\alpha\sin\phi\frac{p_x}{p_z}\cdot y^i \tag{142}$$
$$y \to \sin\alpha\tan\phi\cdot\sigma + \left(1 + \sin\alpha\sin\phi\frac{p_y}{p_z}\right)\cdot y^i + \cos\alpha\sin\phi\frac{p_y}{p_z}\cdot x^i \tag{143}$$

Inverse Lorentz boost. We define the determinat of the inverse Lorentz transformation matrix as

$$D = \frac{1}{\cos\phi} + \tan\phi\left[\frac{p_x^i}{p_z}\cos\alpha + \frac{p_y^i}{p_z}\sin\alpha - \left(1 - \frac{1+\delta^i}{p_z}\right)\sin\phi\right]. \tag{144}$$

$$x \to \frac{1}{D}\Bigg[x\left(\frac{1}{\cos\phi} + \sin\alpha\tan\phi\left(\frac{p_y}{p_z} - \sin\alpha\sin\phi\left(1 - \frac{1+\delta}{p_z}\right)\right)\right) \tag{145}$$

$$+ y\sin\alpha\tan\phi\left(\left(1 - \frac{1+\delta}{p_z}\right)\cos\alpha\sin\phi - \frac{p_x}{p_z}\right) \tag{146}$$

$$- \sigma\tan\phi\left(\cos\alpha + \sin\phi\cos\alpha\sin\alpha\frac{p_y}{p_z} - \sin^2\alpha\sin\phi\frac{p_x}{p_z}\right)\Bigg] \tag{147}$$

$$y \to \frac{1}{D}\Bigg[y\left(\frac{1}{\cos\phi} + \cos\alpha\tan\phi\left(\frac{p_x}{p_z} - \cos\alpha\sin\phi\left(1 - \frac{1+\delta}{p_z}\right)\right)\right) \tag{148}$$

$$+ y\cos\alpha\tan\phi\left(\left(1 - \frac{1+\delta}{p_z}\right)\sin\alpha\sin\phi - \frac{p_y}{p_z}\right) \tag{149}$$

$$- \sigma\tan\phi\left(\sin\alpha + \sin\phi\cos\alpha\sin\alpha\frac{p_x}{p_z} - \cos^2\alpha\sin\phi\frac{p_y}{p_z}\right)\Bigg] \tag{150}$$

$$\sigma \to \frac{1}{D}\Bigg[\sigma\left(1 + \frac{p_x}{p_z}\cos\alpha\sin\phi + \frac{p_y}{p_z}\sin\alpha\sin\phi\right) - x\left(1 + \frac{1+\delta}{p_z}\right)\cos\alpha\sin\phi \tag{151}$$

$$- y\left(1 - \frac{1+\delta}{p_z}\right)\sin\alpha\sin\phi\Bigg] \tag{152}$$

$$\delta \to \delta + \cos\alpha\sin\phi\cdot p_x + \sin\alpha\sin\phi\cdot p_y \tag{153}$$

$$p_x \to p_x + \cos\alpha\sin\phi\cos^3\phi\left[(1+\delta) - p_z^i\right] \tag{154}$$

$$p_y \to p_y + \sin\alpha\sin\phi\cos^3\phi\left[(1+\delta) - p_z^i\right] \tag{155}$$

3.11 RF multipole

The Hamiltonian for a thin RF multipole is

$$H = \delta\left(s - \frac{L}{2}\right)\Bigg\{ - \frac{1}{k_{\mathrm{RF}}}\frac{qV_{\mathrm{RF}}}{p_s c}\cos(\vartheta_{\mathrm{RF}} - k_{\mathrm{RF}}z) + \cdots \tag{156}$$

$$\cdots + \sum_{n=0}^{N}\frac{1}{(n+1)!}\Re\left[(K_{\mathrm{N},n}L\cos(\vartheta_n - k_{\mathrm{RF}}z) + iK_{\mathrm{S},n}L\cos(\varphi_n - k_{\mathrm{RF}}z))(x+iy)^{n+1}\right]\Bigg\} \tag{157}$$

where the n-th order normal- and skew- multipole magnetic strengths are

$$K_{\mathrm{N,n}} = \frac{q}{p_s}\frac{\partial^n B_y}{\partial x^n}, \qquad K_{\mathrm{S,n}} = \frac{q}{p_s}\frac{\partial^n B_x}{\partial x^n}, \tag{158}$$

respectively. The multipolar expansion is done similar as for a static magnetic field, but to account for the oscillatory behaviour the multipolar coefficients are expressed as

$$\tilde{B}_n(z) = \Re[B_n e^{j(\vartheta_n - k_{\mathrm{RF}}z)}] = B_n\cos(\vartheta_n - k_{\mathrm{RF}}z) \tag{159}$$

$$\tilde{A}_n(z) = \Re[A_n e^{j(\varphi_n - k_{\mathrm{RF}}z)}] = A_n\cos(\varphi_n - k_{\mathrm{RF}}z), \tag{160}$$

where ϑ_n and φ_n are the phases for the normal and skew coefficients, $\tilde{B}_n(z)$ and $\tilde{A}_n(z)$, respectively, k_{RF} is the RF wave number of the generating field ($k_{\mathrm{RF}} z = \omega_{\mathrm{RF}} t$).

The kick experienced by an arbitrary particle in (x, y, z) can be expressed as (eq. 16 in [9])

$$\Delta p_x = -\sum_{n=0}^{N} \frac{1}{n!} \Re\left[(K_{\mathrm{N},n} L \cos(\vartheta_n - k_{\mathrm{RF}} z) + i K_{\mathrm{S},n} L \cos(\varphi_n - k_{\mathrm{RF}} z))(x+iy)^n\right], \tag{161}$$

$$\Delta p_y = \sum_{n=0}^{N} \frac{1}{n!} \Im\left[(K_{\mathrm{N},n} L \cos(\vartheta_n - k_{\mathrm{RF}} z) + i K_{\mathrm{S},n} L \cos(\varphi_n - k_{\mathrm{RF}} z))(x+iy)^n\right], \tag{162}$$

$$\Delta p_t = \frac{q V_{\mathrm{RF}}}{p_s c} \sin(\vartheta_{\mathrm{RF}} - k_{\mathrm{RF}} z) + \cdots \tag{163}$$

$$\cdots - k_{\mathrm{RF}} \sum_{n=0}^{N} \Re\left[(K_{\mathrm{N},n} L \sin(\vartheta_n - k_{\mathrm{RF}} z) + i K_{\mathrm{S},n} L \sin(\varphi_n - k_{\mathrm{RF}} z))(x+iy)^n\right]. \tag{164}$$

Temporarily in Sixtrack the following equations are used:

$$\Delta p_x = b_2\, x\, \cos(\phi + k\, z) \tag{165}$$
$$\Delta p_y = -b_2\, y\, \cos(\phi + k\, z) \tag{166}$$
$$\Delta \delta = -k\, \frac{b_2}{2}\, \left(x^2 - y^2\right) \sin(\phi + k\, z) \tag{167}$$

$$\Delta p_x = b_3\, \left(x^2 - y^2\right) \cos(\phi + k\, z) \tag{168}$$
$$\Delta p_y = -2 b_3\, x y\, \cos(\phi + k\, z) \tag{169}$$
$$\Delta \delta = -k\, \frac{b_3}{3}\, \left(x^3 - 3 x y^2\right) \sin(\phi + k\, z) \tag{170}$$

$$\Delta p_x = b_4\, \left(x^3 - 3 x y^2\right) \cos(\phi + k\, z) \tag{171}$$
$$\Delta p_y = -b_4\, \left(3 x^2 y - y^3\right) \cos(\phi + k\, z) \tag{172}$$
$$\Delta \delta = -k\, \frac{b_4}{4}\, \left(x^4 - 6 x^2 y^2 + y^4\right) \sin(\phi + k\, z) \tag{173}$$

$$\Delta p_x = a_2\, y\, \cos(\phi + k\, z) \tag{174}$$
$$\Delta p_y = a_2\, x\, \cos(\phi + k\, z) \tag{175}$$
$$\Delta \delta = -k\, a_2\, x y\, \sin(\phi + k\, z) \tag{176}$$

$$\Delta p_x = 2a_3\, xy\, \cos\left(\phi + k\, z\right) \tag{177}$$
$$\Delta p_y = -a_3\, \left(y^2 - x^2\right)\, \cos\left(\phi + k\, z\right) \tag{178}$$
$$\Delta\delta = k\, \frac{a_3}{3}\, \left(y^3 - 3yx^2\right)\, \sin\left(\phi + k\, z\right) \tag{179}$$

$$\Delta p_x = a_4\, \left(y^3 - 3yx^2\right)\, \cos\left(\phi + k\, z\right) \tag{180}$$
$$\Delta p_y = a_4\, \left(3xy^2 - x^3\right)\, \cos\left(\phi + k\, z\right) \tag{181}$$
$$\Delta\delta = -k\, a_4\, \left(x^3 y - y^3 x\right)\, \sin\left(\phi + k\, z\right) \tag{182}$$

3.12 Phase-trombone, matrix element

The linear “phase trombone" allows to introduce a change in the transverse phases without spoiling the linear optics of the rest of the machine, i.e. the Twiss parameters are the same at entrance and exit of the element. The effect of the element is contained in the matrix M. An addition to the closed orbit can be done through the elements $(x_{co}, x'_{co}, y_{co}, y'_{co}, \sigma_{co})$.

$$\sigma \to \sigma + \sigma_{co} + M_{51} \cdot x + M_{52} \cdot x' + M_{53} \cdot y + M_{54} \cdot y' + M_{56} \cdot \delta \tag{183}$$
$$x \to x_{co} + M_{11} \cdot x + M_{12} \cdot x' + M_{16} \cdot \delta \tag{184}$$
$$x' \to x'_{co} + M_{21} \cdot x + M_{22} \cdot x' + M_{26} \cdot \delta \tag{185}$$
$$y \to y_{co} + M_{33} \cdot y + M_{34} \cdot y' + M_{36} \cdot \delta \tag{186}$$
$$y' \to y'_{co} + M_{43} \cdot y + M_{44} \cdot y' + M_{46} \cdot \delta \tag{187}$$

3.13 Wire

The wire element is described by in total 7 parameters: the wire current I, the physical length of the wire L and the length of the embedded drift L_{emb}, the horizontal distance dx and vertical distance dy between the wire midpoint and the closed orbit, and the tilt angle ϕ in the (z, y) plane and the tilt angle θ in the (x, z) plane. The length L is the physical length of the wire while the embedded drift is the length of the integration interval of the kick (Eqn. 194) in order to also take the fringe fields of the wire into account. This is illustrated in Fig. 2 which shows the vector potential and magnetic field together with the physical length L and the length of the embedded drift L_{emb}. The tilt angles are illustrated in Fig. 3.

To calculate the kick strength $\mathcal{L}$ of the wire in order to compensate the beam-beam kick from one long-range beam-beam encounter, the following relation between holds [11]:

$$\mathcal{L} = e \cdot c \cdot N_p = L \cdot I \tag{188}$$

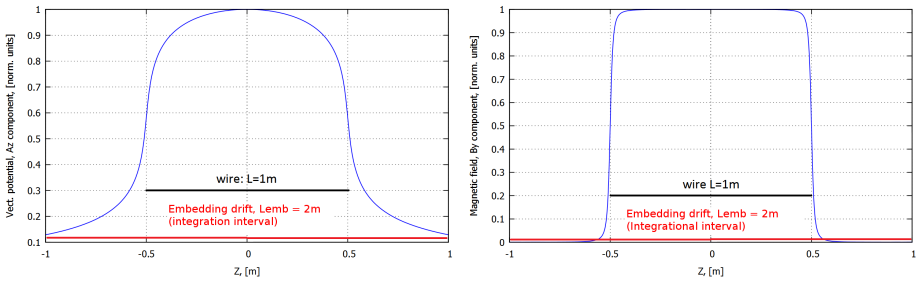

Figure 2: Vector potential (left) and magnetic field (right) of a current bearing wire with physical length $L = 1$ m and embedded drift (integrational length) $L_{\text{emb}} = 2$ m.

with N_p being the bunch charge and L and I are the length and current of the wire. $\mathcal{L}$ than has to units Am.

The generic formula for a vector potential of a straight current bearing wire with length L and current I centered at the origin is given in Cartesian coordinates by the following expression[1]:

$$A_i(x,y,z) = \frac{I\mu_0 \cos(c_i)}{4\pi} \cdot \left(\operatorname{asinh}\left(\frac{L/2-a}{\sqrt{b-a^2}}\right) - \operatorname{asinh}\left(\frac{-L/2-a}{\sqrt{b-a^2}}\right)\right), \; i = x,y,z, \tag{189}$$

where the parameters a and b are defined as

$$a = x \cdot \cos(c_x) + y \cdot \cos(c_y) + z \cdot \cos(c_z), \tag{190}$$

$$b = x^2 + y^2 + z^2, \tag{191}$$

and $\cos(c_i)$ are the direction cosines. The direction cosines can in general be expressed through two tilt angles ϕ and θ (see Fig. 3) with:

$$\begin{aligned} \cos(c_x) &:= \frac{\tan(\phi)}{\sqrt{\tan^2(\phi)+\tan^2(\theta)+1}} \\ \cos(c_y) &:= \frac{\tan(\theta)}{\sqrt{\tan^2(\phi)+\tan^2(\theta)+1}} \\ \cos(c_z) &:= \frac{1}{\sqrt{\tan^2(\phi)+\tan^2(\theta)+1}}. \end{aligned} \tag{192}$$

In case the wire lies parallel to the longitudinal axis ($\phi = \theta = 0$), the transverse potential $A_{x,y}$ vanish and the longitudinal potential can be further

[1] Note that Curvilinear and Cartesian coordinate system are equivalent as the curvature is zero at the location of the wire element.

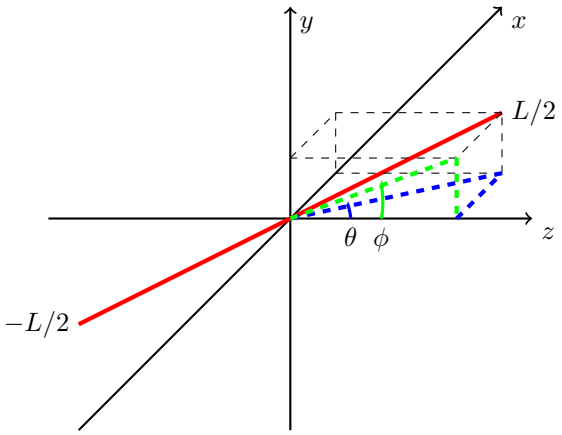

Figure 3: Wire centered (red) at the origin including the angles ϕ and θ as defined for the directional cosines in Eqn. 192.

simplified, leading to:

$$\begin{aligned} A_x(x,y,z) &= 0 \\ A_y(x,y,z) &= 0 \\ A_z(x,y,z) &= \frac{I\mu_0}{4\pi} \cdot \left(\operatorname{asinh}\left(\frac{L/2 - z}{\sqrt{x^2+y^2}} \right) - \operatorname{asinh}\left(\frac{-L/2 - z}{\sqrt{x^2+y^2}} \right) \right) \end{aligned} \tag{193}$$

The Hamiltonian for the wire is then simply $H = -A_s = -A_z$.

The kick experienced by an arbitrary particle with coordinates (x, y, z) using a first order symplectic integrator is then given by:

$$\Delta p_x = \int_{-L_{\text{emb}}/2}^{+L_{\text{emb}}/2} \frac{\partial A_z(x,y,s)}{\partial x} ds, \tag{194}$$

$$\Delta p_y = \int_{-L_{\text{emb}}/2}^{+L_{\text{emb}}/2} \frac{\partial A_z(x,y,s)}{\partial y} ds, \tag{195}$$

$$\Delta x = \Delta y = \Delta \delta = \Delta \sigma = 0 \tag{196}$$

where L_{emb} is the embedding drift or integration length (see Fig. 2), which takes into account the fringe field of the wire, while the parameter L in Eqn. 193 denotes the physical length of the wire. A symplectic rotation of the coordinate system as described in [10] is included in order to compute the transport map for arbitrary orientation, explicitly arbitrary angles θ and ϕ in Fig. 3.

The first order symplectic transport map in thin lens approximation for an arbitrary orientation of the wire can then be obtained by the following steps:

Step 1 Shift to the origin: We define the new variables

$$\begin{aligned} r_x &:= x - x_{co} + dx \\ r_y &:= y - y_{co} + dy \end{aligned} \tag{197}$$

where x_{co} and y_{co} denotes the closed orbit at the center of the wire.

Step 2 Symplectic rotation in (x, z) by θ as described in [10]: In a drift space the normalized momenta p_i are related by $p_x^2 + p_y^2 + p_z^2 = (1+\delta)^2$ and we can thus write p_z as

$$p_z = \sqrt{(1+\delta)^2 - p_x^2 - p_y^2} \tag{198}$$

The rotation by θ can then be expressed as a rotation first in (p_x, p_z):

$$\begin{aligned} p_x &\to p_x \cdot \cos\theta + p_z \cdot \sin\theta \\ p_z &\to -p_x \cdot \sin\theta + p_z \cdot \cos\theta \end{aligned} \tag{199}$$

followed by a transformation in (r_x, r_y):

$$\begin{aligned} r_x &\to r_x \left(\cos\theta - \frac{p_x}{p_z} \cdot \sin\theta \right) \\ r_y &\to r_y - r_x \cdot \frac{p_y}{p_z} \cdot \sin\theta \end{aligned} \tag{200}$$

Step 3 Symplectic rotation in (y, z) by ϕ as described in [10]: The new p_z is again defined as $p_z = \sqrt{(1+\delta)^2 - p_x^2 - p_y^2}$ using the updated values of p_x, p_y from Step 2. Analogical to the symplectic rotation in (x, z), the rotation by ϕ in (y, z) can be expressed as a rotation first in (p_y, p_z):

$$\begin{aligned} p_y &\to p_y \cdot \cos\phi + p_z \cdot \sin\phi \\ p_z &\to -p_y \cdot \sin\phi + p_z \cdot \cos\phi \end{aligned} \tag{201}$$

followed by a transformation in (r_x, r_y):

$$\begin{aligned} r_x &\to r_x - r_y \cdot \frac{p_x}{p_z} \cdot \sin\phi \\ r_y &\to r_y \left(\cos\theta - \frac{p_y}{p_z} \sin\theta \right) \end{aligned} \tag{202}$$

Step 4 Application of the symplectic kick of a wire aligned along the longitudinal axis ($\theta = \phi = 0$): We define the radius r in the (r_x, r_y) by:

$$r^2 := r_x^2 + r_y^2 \tag{203}$$

The thin lens kick of the wire aligned along the longitudinal axis can then be expressed by:

$$\begin{aligned} p_x &\to p_x - 10^{-7} \cdot I \frac{e}{P_0} \frac{r_x}{r^2} \left(d^+ - d^-\right) - p_{co,wire} \\ p_y &\to p_y - 10^{-7} \cdot I \frac{e}{P_0} \frac{r_y}{r^2} \left(d^+ - d^-\right) - p_{co,wire} \end{aligned} \tag{204}$$

with d^+ and d^- defined as:

$$d^+ = \sqrt{(L_{\text{emb}} + L)^2 + 4r^2} \tag{205}$$

$$d^- = \sqrt{(L_{\text{emb}} - L)^2 + 4r^2} \tag{206}$$

As reminder L denotes the physical length of the wire and L_{emb} the length of the embedded drift. The parameter $p_{co,wire}$ is the closed orbit kick due to the wire. This kick is only subtracted if *ibeco* is equal to 1 in the BEAM block.

Step 5 Backward rotation by $-\phi$ in (p_y, p_z): The new p_z is again defined as $p_z = \sqrt{(1+\delta)^2 - p_x^2 - p_y^2}$ using the updated values of p_x, p_y from Step 4. The rotation is then given by:

$$\begin{aligned} p_y &\to p_y \cdot \cos\phi - p_z \cdot \sin\phi \\ p_z &\to p_y \cdot \sin\phi + p_z \cdot \cos\phi \end{aligned} \tag{207}$$

Step 6 Backward rotation by $-\theta$ in (p_x, p_z): The new p_z is again defined as $p_z = \sqrt{(1+\delta)^2 - p_x^2 - p_y^2}$ using the updated values of p_x, p_y from Step 5. The rotation is then given by:

$$\begin{aligned} p_x &\to p_x \cdot \cos\theta - p_z \cdot \sin\theta \\ p_z &\to p_x \cdot \sin\theta + p_z \cdot \cos\theta \end{aligned} \tag{208}$$

Note that as required for a thin lens approximation, the map does not change x and y.

3.14 Crab cavity

The voltage of the crab cavity is denoted by V, the frequency by f and the phase by ϕ. The map for a horizontal crab cavity is

$$p_x \to p_x - \frac{V}{p} \cdot (1+\delta) \sin\left(2\pi f \frac{\sigma}{c} + \phi\right) \tag{209}$$

$$\delta \to \delta - 2\pi f \frac{V}{pc} \cdot x \cdot \cos\left(2\pi f \frac{\sigma}{c} + \phi\right). \tag{210}$$

Followed by updates of the momentum and energy due to the change of δ. The map for a vertical crab cavity is given by replacing $x \to y$ and $p_x \to p_y$ in the map above.

3.15 AC-dipole

The excitation amplitude of the AC-dipole is denoted by A [Tm], the excitation frequency by q_d [2π] and the phase of the excitation by ϕ. The map presented here is for a purely horizontal dipole, the map for a vertical dipole is obtained by replacing $p_x \to p_y$.

The effect of the AC-dipole is split into four stages. The turn number is denoted by n.

1. A number of free turns n_{free}, in which the AC-dipole has no effect on the motion.

2. Ramp-up of the voltage from 0 to the excitation amplitude A for $n_{\text{ramp-up}}$ turns.

$$n' = \frac{n - n_{\text{free}}}{n_{\text{ramp-up}}} \tag{211}$$

$$p_x \to p_x + n' \cdot \frac{A}{pc} \cdot (1+\delta) \sin\left(2\pi q_d \cdot (n - n_{\text{free}}) + \phi\right) \tag{212}$$

3. Constant excitation amplitude for n_{flat} turns.

$$p_x \to p_x + \frac{A}{pc} \cdot (1+\delta) \sin\left(2\pi q_d \cdot (n - n_{\text{free}}) + \phi\right) \tag{213}$$

4. Ramp-down of the voltage from the excitation amplitude A to 0 for $n_{\text{ramp-down}}$ turns.

$$n' = \frac{n - n_{\text{free}} - n_{\text{ramp-up}} - n_{\text{flat}} - n_{\text{ramp-down}}}{n_{\text{ramp-down}}} \tag{214}$$

$$p_x \to p_x + n' \cdot \frac{A}{p} \cdot (1+\delta) \sin\left(2\pi q_d \cdot (n - n_{\text{free}}) + \phi\right) \tag{215}$$

3.16 Electron lens

3.16.1 Hollow electron lens - uniform annular profile

For a uniform distribution of the electron beam between R_1 and R_2, the radial kick can be described by a shape function $f(r)$ and a maximum kick strength θ_{max}:

$$\theta(r) = \frac{f(r)}{(r/R_2)} \cdot \theta_{\text{max}} \tag{216}$$

with $r = \sqrt{x^2 + y^2}$ and θ_{max} independent of r. The shape function $f(r)$ is defined as

$$f(r) = \frac{I(r)}{I_T} = \frac{2\pi}{I_T} \int_0^r r\rho(r)\mathrm{d}r \tag{217}$$

where I_T is the total electron beam current, $I(r)$ is the current enclosed in a radius r and $\rho(r)$ is the electron beam density distribution.

For a uniform profile one then obtains:

$$f(r) = \begin{cases} 0 & , \quad r < R_1 \\ \frac{r^2 - R_1^2}{R_2^2 - R_1^2} & , \quad R_1 \leq r < R_2 \\ 1 & , \quad R_2 \leq r \end{cases} \tag{218}$$

and

$$\theta_{\max} = \theta(R_2) = \frac{2LI_T(1 \pm \beta_e\beta_p)}{4\pi\epsilon_0 \left(B\rho\right)_p \beta_e\beta_p c^2} \cdot \frac{1}{R_2} \tag{219}$$

where L is the length of the e-lens, I_T the total electron beam current, β_e and β_p the relativistic β of electron and proton beam, $B\rho$ the magnetic rigidity, c the speed of light and ϵ_0 the vacuum permittivity. The $\pm$-sign represents the two cases of the electron beam traveling in the direction of the proton beam ($v_e v_p > 0$) leading to "$-$" or in the opposite direction ($v_e v_p < 0$) leading to "$+$". For hollow electron beam collimation, electron and proton beam travel in opposite directions.

The kick in (x', y') can then be expressed as (note $\frac{x}{r} = \cos(\phi)$, $\frac{y}{r} = \sin(\phi)$):

$$x' = x' - \theta_{\max} \cdot \frac{R_2}{r^2} \cdot f(r) \cdot x \cdot \frac{1}{1+\delta} \tag{220}$$

$$y' = y' - \theta_{\max} \cdot \frac{R_2}{r^2} \cdot f(r) \cdot y \cdot \frac{1}{1+\delta} \tag{221}$$

If the electron lens is offset by $(x_{\text{offset}}, y_{\text{offset}})$, the coordinates (x, y) are simply transfered to:

$$\tilde{x} = x + x_{\text{offset}} \tag{222}$$

$$\tilde{y} = y + y_{\text{offset}} \tag{223}$$

$$\tilde{r} = \sqrt{\tilde{x}^2 + \tilde{y}^2} \tag{224}$$

and the kick is then given by:

$$x' = x' - \theta_{\max} \cdot \frac{r_2}{\tilde{r}^2} \cdot f(\tilde{r}) \cdot \tilde{x} \tag{225}$$

$$y' = y' - \theta_{\max} \cdot \frac{r_2}{\tilde{r}^2} \cdot f(\tilde{r}) \cdot \tilde{y} \tag{226}$$

This idealized implementation of the hollow e-lens has no explicit dependence on the particle energy. The particle energy is only taken into account in form of the input parameter $\theta_{\max}$ provided by the user. A change of the particle energy could occur if the particle enters with an initial x' or y' and thus sees an accelerating or respectively decelerating field.

3.17 Misalignment

Misalignments of elements affects the coordinates at the entrance of an element as follows

$$x \to (x - x_s) \cdot t_c + (y - y_s) \cdot t_s \tag{227}$$

$$y \to -(x - x_s) \cdot t_s + (y - y_s) \cdot t_c, \tag{228}$$

where x_s and y_s are the displacements in the horizontal and vertical directions, respectively. t_c and t_s are the cosine and sine of the tilt angle for the element.

4 Optics calculations

Optics calculation are needed to study the motion around the closed orbit. By defining z as the vector of $2k$ coordinates,

$$z = (z_1, \ldots, z_{2k})^T = (x - x_0, p_x - p_{x0}, y - y_0, p_y - p_{y0}, \tau - \tau_0, p_t - p_{t0})^T \tag{229}$$

one can define linear transfer maps (e.g. $M_{1\to 2}$ that propagates coordinates between two points s_1, s_2) and the one-turn map (e.g. M_1 that combines the effects for one turn starting from s_1):

$$z(s_2) = M_{1\to 2} z(s_1) \qquad\qquad z(C + s_1) = M_1 z(s_1). \tag{230}$$

In the following we will describe the optics calculation based on the Ripken formalism described in [12]. A good summary is also given in the MAD8 physics manual [13].

4.1 Diagonalisation of one-turn matrix

Since the matrices derive from symplectic maps, the eigenvalue spectrum of the one-turn map M consists of $2k$ distinct eigenvalues and linearly independent eigenvectors. In addition, for the motion to be stable the eigenvalues $\lambda_k^{\pm}$ with eigenvectors $v_k^{\pm}$ have to be complex [12]:

$$M v_k^{\pm} = \lambda_k^{\pm} v_k^{\pm},\ k = 1, \ldots, 3 \tag{231}$$

$$v_k^{+} = (v_k^{-})^*, \quad \lambda_k^{+} = (\lambda_k^{-})^*, \quad |\lambda_k^{\pm}| = 1 \tag{232}$$

As the eigenvectors are linearly independent M can be diagonalized with

$$M = V \Lambda V^{-1}, \tag{233}$$

where V consists of the eigenvectors and Λ of the eigenvalues:

$$V = \begin{pmatrix} v_{1,1}^{+} & v_{1,1}^{-} & \cdots & v_{3,1}^{-} \\ v_{1,2}^{+} & v_{1,2}^{-} & \cdots & v_{3,2}^{-} \\ \vdots & \vdots & \vdots & \vdots \end{pmatrix} \qquad \Lambda = \begin{pmatrix} \lambda_1^{+} & & & \\ & \lambda_1^{-} & & \\ & & \ddots & \\ & & & \lambda_3^{-} \end{pmatrix} \tag{234}$$

for which $v_{i,j}^{\pm}$ is the component j of eigenvector $v_i^{\pm}$.

The same calculation can be carried out with real numbers by the following definitions:

$$v_k^{\pm} = a_k \pm i b_k, \qquad \lambda_k^{\pm} = \cos\mu_k \pm i \sin\mu_k, \qquad \mu_k, a_k, b_k \in \mathbb{R} \tag{235}$$

such that:

$$M = WRW^{-1} \tag{236}$$

with

$$R = R(\mu_k) = \begin{pmatrix} \cos\mu_1 & \sin\mu_1 & & & & \\ -\sin\mu_1 & \cos\mu_1 & & & & \\ & & \ddots & & & \\ & & & \cos\mu_3 & \sin\mu_3 \\ & & & -\sin\mu_3 & \cos\mu_3 \end{pmatrix}, \tag{237}$$

$$W = \begin{pmatrix} a_{1,1} & b_{1,1} & \cdots & a_{3,1} & b_{3,1} \\ a_{1,2} & b_{1,2} & \cdots & a_{3,2} & b_{3,2} \\ \vdots & \vdots & \vdots & \vdots & \\ a_{1,6} & b_{1,6} & \cdots & a_{3,6} & b_{3,6} \end{pmatrix} \tag{238}$$

Usually μ_k is written as $\mu_k = 2\pi Q_k$, where Q_k is then the tune of the mode k.

4.2 Normalisation of eigenvectors

By convention, the eigenvectors and values are normalized, sorted and rotated so that the following three conditions are fulfilled:

1. Plane 1 is associated with the horizontal, plane 2 with the vertical and plane 3 with the longitudinal plane. This is achieved by first normalizing the eigenvectors $v_k^{\pm}$ and then sorting them so that:

$$|v^+_{j,2j-1}| = |v^-_{j,2j-1}| = \max_{k=1,2,3} v_{k,j}, \quad j = 1, \ldots, 3 \tag{239}$$

2. The eigenvectors are then rotated with a phase term ψ_k

$$v_k \to v_k \exp(i\psi_k) \tag{240}$$

such that

$$\text{angle}(v^+_{k,2k-1}) = 0 \leftrightarrow \psi_k = -\text{angle}(v^+_{k,2k-1}) \tag{241}$$

In real space, Eqn. 239 and 241 then become equivalent to:

$$|a_{j,2j-1}| = \max_{k=1,2,3} |a_{k,j}|, \qquad b_{j,2j-1} = 0, \qquad j = 1, \ldots, 3 \tag{242}$$

This has the effect that a particle with $x = 0$ is transformed to $\tilde{x}$ in the normalized phase space.

3. The sign of $b_{k,j}$ is fixed by the symplectic condition on W

$$W^T S W = S \tag{243}$$

with S defined as

$$S = \begin{pmatrix} 0 & 1 & & \\ -1 & 0 & & \\ & & \ddots & \end{pmatrix} \tag{244}$$

which is equivalent to:

$$\begin{aligned} &a_k^T \cdot S \cdot b_k = 1, \quad b_k^T \cdot S \cdot a_k = -1, && \text{for } k = l \\ &a_k^T \cdot S \cdot b_l = 0, && \text{for } k \neq l \\ &a_k^T \cdot S \cdot a_l = 0, \quad b_k^T \cdot S \cdot b_l = 0, && k, l = 1, \ldots, 3 \end{aligned} \tag{245}$$

Eqn. 245 yields that in phase space a_k is thus obtained by an anticlockwise rotation of b_k by $\pi/2$ and a scaling of its length with $|a_k| = \frac{1}{|b_k|}$.

4.3 Conversion to normalized coordinates

We will show in the following that in the normalized phase space the propagation of particle coordinates $z(s)$ from s_1 to s_2 is just a rotation by an angle ϕ_k in the $k = 1, \ldots, 3$ planes, while the amplitude I_k and initial phase $\phi_{k,0}$ stay constant, explicitly $z(s)$ is then given by:

$$z(s) = \sum_{k=1}^{3} \sqrt{2I_k} \left(a_k(s) \cos\left(\phi_{k,0} + \phi_k(s)\right) - b_k(s) \sin\left(\phi_{k,0} + \phi_k(s)\right)\right) \tag{246}$$

and

$$\begin{aligned} z(s_2) = W(s_2) R(\phi_k) W(s_1)^{-1} z(s_1), \\ \text{with } \phi_k = \phi_k(s_2) - \phi_k(s_1) \end{aligned} \tag{247}$$

This implies that one turn is simply a rotation by $\phi_k = 2\pi Q_k$ where Q_k is the tune of the mode k. In the transverse plane the tune ($Q_{I,II}$) is usually positive and the particles rotate clockwise, while in the longitudinal plane the tune (Q_{III}) is negative above γ_T leading to an anticlockwise rotation.

For the derivation the following steps are needed:

1. The effect of one turn on the normalized variable $\tilde{z}(s) = W^{-1}(s) z(s)$ is a rotation:

$$\tilde{z}(C + s) = W^{-1} z(s + C) \overset{\text{(Eqn.236)}}{=} W^{-1} W R W^{-1} z(s) = R \tilde{z}(s), \tag{248}$$

As M and R are symplectic also W is symplectic, and its inverse is thus given by $S^{-1} W^T S$, explicitly:

$$W^{-1} = \begin{pmatrix} b_{12} & -b_{11} & b_{14} & -b_{13} & b_{16} & -b_{15} \\ -a_{12} & a_{11} & -a_{14} & a_{13} & -a_{16} & a_{15} \\ b_{22} & -b_{21} & b_{24} & -b_{23} & b_{26} & -b_{25} \\ -a_{22} & a_{21} & -a_{24} & a_{23} & -a_{26} & a_{25} \\ b_{32} & -b_{31} & b_{34} & -b_{33} & b_{36} & -b_{35} \\ -a_{32} & a_{31} & -a_{34} & a_{33} & -a_{36} & a_{35} \end{pmatrix} \tag{249}$$

2. The one-turn map and W-matrix can be propagated from s_1 to s_2 by

$$M_2 = M_{1\to 2} M_1 M_{1\to 2}^{-1} \qquad W_2 = M_{1\to 2} W_1 \tag{250}$$

As Eqn. 248 represents a similarity transformation, the eigenvalues are thus independent of the position s and as the rotation matrix R consists of the eigenvalues of M, the angle of the rotation $\mu_k = 2\pi Q_k$ is thus also independent of s.

3. As Eqn. 236 represents a basis transformation from the standard $\mathbb{R}^2$ basis to the eigenvector basis, the vectors a_k and b_k are projected onto (Eqn. 245):

$$\begin{aligned}
\tilde{a}_1 = W^{-1} a_1 &= -SW^T S a_1 \\
&= -S(a_1 S a_1, b_1 S a_1, \ldots, b_3 S a_1)^T = (1, 0, \ldots, 0) \\
\tilde{b}_1 = W^{-1} b_1 &= -SW^T S b_1 \\
&= -S(a_1 S b_1, b_1 S b_1, \ldots, b_3 S b_1)^T = (0, 1, \ldots, 0) \\
&\ldots \\
\tilde{b}_3 = W^{-1} b_3 &= -SW^T S b_3 \\
&= -S(a_1 S b_3, b_1 S b_3, \ldots, b_3 S b_3)^T = (0, 0, \ldots, 1)
\end{aligned} \tag{251}$$

in the normalized phase space.

4. From Eqn. 248 it follows that the amplitude I_k and initial phase ϕ_{k0} of $\tilde{z} = W^{-1} z = (\tilde{z}_{a_1}, \tilde{z}_{b_1}, \ldots, \tilde{z}_{b_3})$

$$I_k = \frac{(\tilde{z}_{a_k})^2 + (\tilde{z}_{b_k})^2}{2}, \quad k = 1, \ldots, 3 \tag{252}$$

$$\tan \phi_{k0} = -\frac{\tilde{z}_{b_k}}{\tilde{z}_{a_k}} \tag{253}$$

are constants of the motion, which is illustrated in Fig. 4. The initial

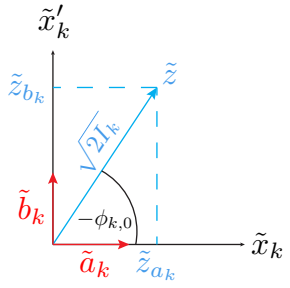

Figure 4: Normalized phase space.

phase is defined with a minus sign in view of the definition of the Twiss

parameters, where the initial phase is then added (and not subtracted) to the phase advance. The components of $\tilde{z}$ are then explicitly given by:

$$\tilde{z}_{a_k} = \sum_{j=1}^{3} b_{k,2j}\, z_{2j-1} - b_{k,2j-1}\, z_{2j}, \quad k = 1, \ldots, 3 \tag{254}$$

$$\tilde{z}_{b_k} = \sum_{j=1}^{3} a_{k,2j-1}\, z_{2j} - a_{k,2j}\, z_{2j-1}, \quad k = 1, \ldots, 3. \tag{255}$$

An arbitrary vector $z(s)$ can thus be written in the following form:

$$\begin{aligned} z(s) &= W(s)\tilde{z}(s) \\ &= W(s) \left(\sum_{k=1}^{3} \tilde{z}_{a_k} \tilde{a}_k + \tilde{z}_{b_k} \tilde{b}_k \right) \\ &= \sum_{k=1}^{3} \tilde{z}_{a_k} W(s) \tilde{a}_k + \tilde{z}_{b_k} W(s) \tilde{b}_k \overset{\text{Eqn. } 251}{=} \sum_{k=1}^{3} \tilde{z}_{a_k} a_k + \tilde{z}_{b_k} b_k \\ &\overset{\text{Eqns. } 252,253}{=} \sum_{k=1}^{3} \sqrt{2I_k}\, (a_k \cos\phi_{k0} - b_k \sin\phi_{k0}) \end{aligned} \tag{256}$$

4.4 Twiss parameters

In the following the parameter k will always be used for the mode k and the parameter $j = 1, 2, 3$ for the horizontal (x, x'), vertical (y, y') and longitudinal plane (σ, δ) in the phase space. z_{2j-1} then stands for the coordinates (x, y, σ) and z_{2j} for (x', y', δ).

The Twiss parameters can be introduced by writing the components of the eigenvector basis $(a_k(s), b_k(s))$ as the product of two envelope functions $\sqrt{\beta_{k,j}(s)}$, $\sqrt{\gamma_{k,j}(s)}$ and phase functions $\phi_{k,j}(s)$, $\bar{\phi}_{k,j}(s)$, also called Twiss parameters or lattice functions, with

$$\begin{aligned} a_{k,2j-1}(s) &= \sqrt{\beta_{k,j}(s)} \cos\phi_{k,j}(s), \\ b_{k,2j-1}(s) &= \sqrt{\beta_{k,j}(s)} \sin\phi_{k,j}(s), \;\; k, j = 1, \ldots, 3, \end{aligned} \tag{257}$$

$$\begin{aligned} a_{k,2j}(s) &= \sqrt{\gamma_{k,j}(s)} \cos\bar{\phi}_{k,j}(s), \\ b_{k,2j}(s) &= \sqrt{\gamma_{k,j}(s)} \sin\bar{\phi}_{k,j}(s), \;\; k, j = 1, \ldots, 3 \end{aligned} \tag{258}$$

where $\beta_{k,j}(s), \alpha_{k,j}(s), \gamma_{k,j}(s)$ represent the projection of the ellipse of mode k on the plane of coordinates $z_{2k-1} - z_{2k}$ (see Fig. 5)

Using Eqns. 246, 257, 258 and $\cos(x + y) = \cos x \cos y - \sin x \sin y$, the

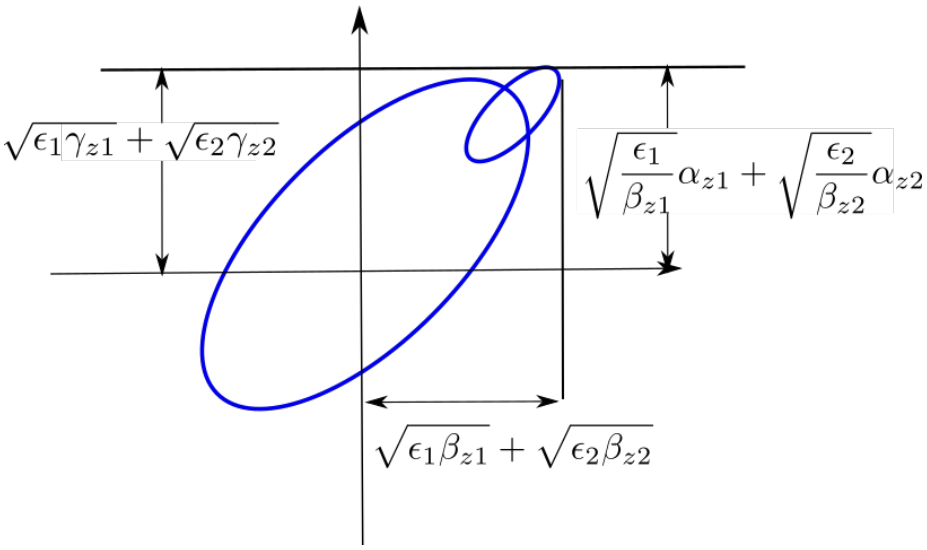

Figure 5: Projection of lattice function in the $z - z'$ plane.

coordinates $z(s)$ can be expressed by:

$$z_{2j-1}(s) = \sum_{k=1}^{3} \sqrt{2I_k\beta_{k,j}(s)}\cos\left(\phi_{k,j}(s) + \phi_{k,0}\right) \tag{259}$$

$$z_{2j}(s) = \sum_{k=1}^{3} \sqrt{2I_k\gamma_{k,j}(s)}\cos\left(\bar{\phi}_{k,j}(s) + \phi_{k,0}\right),\ j = 1, \ldots, 3 \tag{260}$$

Conversely the lattice functions can also be expressed by a_k and b_k with

$$\beta_{k,j}(s) = a_{k,2j-1}(s)^2 + b_{k,2j-1}(s)^2 \tag{261}$$

$$\alpha_{k,j}(s) = a_{k,2j-1}(s)a_{k,2j}(s) - b_{k,2j-1}(s)b_{k,2j}(s) \tag{262}$$

$$\gamma_{k,j}(s) = a_{k,2j}(s)^2 + b_{k,2j}(s)^2, \tag{263}$$

The well known relations between the lattice functions

$$\sum_{j=1}^{3} \beta_{k,j}\phi'_{k,j} = 1 \tag{264}$$

$$\gamma_{k,j} = \frac{\beta_{k,j}^2\phi_{k,j}'^2 + \alpha_{k,j}^2}{\beta_{k,j}}, \text{ with} \tag{265}$$

$$\alpha_{k,j} := -\frac{1}{2}\beta'_{k,j} \tag{266}$$

can then be derived with the help of the normalization condition (Eqn. 245)

$$a_k^T S b_k = 1 \tag{267}$$

by the following steps:

1. As $x' = \frac{dx}{ds}$, $y' = \frac{dy}{ds}$ and $\delta = \frac{d\sigma}{ds}$ the following relations hold also for a_k and b_k:

$$a_{k,2j} = a'_{k,2j-1} = \frac{d}{ds}(a_{k,2j-1}), \tag{268}$$

$$b_{k,2j} = b'_{k,2j-1} = \frac{d}{ds}(b_{k,2j-1}),\ k,j = 1,\ldots,3 \tag{269}$$

2. The normalization condition Eqn. 245 can then be written as

$$\begin{aligned} a_k^T S b_k &= \sum_{j=1}^{3} \sqrt{\beta_{k,j}}\cos\phi_{k,j}\left(\sqrt{\beta_{k,j}}\sin\phi_{k,j}\right)' \\ &\quad - \left(\sqrt{\beta_{k,j}}\cos\phi_{k,j}\right)'\sqrt{\beta_{k,j}}\sin\phi_{k,j} \\ &= \sum_{j=1}^{3}\beta_{k,j}\phi'_{k,j} \\ &= 1 \end{aligned} \tag{270}$$

   Note that Eqn. 270 yields the the following relation between the phase advance ϕ and β in 2D:

$$\phi(s) = \phi(0) + \int_{s_0}^{s} \frac{1}{\beta(\bar{s})} d\bar{s} \tag{271}$$

3. Using the abbreviation $\alpha_{k,j} := -\frac{1}{2}\beta_{k,j}$, one finds for each mode k and plane j

$$\sqrt{\gamma_{k,j}}\cos\phi_{k,j} = a_{k,2j} = a'_{k,2j-1} = (\sqrt{\beta_{k,j}}\cos\phi_{k,j})' \tag{1}$$

$$\sqrt{\gamma_{k,j}}\sin\phi_{k,j} = b_{k,2j} = b'_{k,2j-1} = (\sqrt{\beta_{k,j}}\sin\phi_{k,j})' \tag{2}$$

$$\overset{(1)^2+(2)^2}{\Rightarrow} \gamma_{k,j} = \frac{\beta_{k,j}^2\phi_{k,j}'^2 + \alpha_{k,j}^2}{\beta_{k,j}}, \quad k,j = 1,\ldots,3 \tag{272}$$

which simplifies in the 2D case to:

$$\gamma \overset{\text{Eqn. 270}}{=} \frac{1+\alpha^2}{\beta} \tag{273}$$

5 Table of symbols

$\vec{R}$: moving reference frame origin

s: path length of the reference frame origin trajectory

$\hat{X}, \hat{Y}, \hat{Z}$: global reference frame bases

X, Y, Z: reference frame origin coordinates $\vec{R}(s) = X(s)\hat{X} + Y(s)\hat{Y} + Z(s)\hat{Z}$

$\vec{Q}$: particle position

$\hat{x}, \hat{y}, \hat{s}$: moving reference frame bases

x, y: transverse particle coordinates $\vec{Q}(s) = \vec{R}(s) + x(s)\,\hat{x}(s) + y(s)\,\hat{y}(s)$

$t(s)$: time at which the particle is located in the plane $\hat{x}(s), \hat{y}(s)$

v, P, E, m, q: particle velocity momenta, energy, rest mass, charge

v_0, P_0, E_0, m_0, q_0: reference momentum, energy, rest mass,

β_0, γ_0: reference relativistic factors

$\Delta t = s/\beta_0 - ct$: Mad time deviation, canonical conjugate of p_t

$\sigma = s - \beta_0 ct$: Sixtrack time deviation, canonical conjugate of p_σ

$\Delta s = s - \beta ct$ path length deviation, canonical conjugate of δ

$z = \beta(s/\beta_0 - ct)$ John time deviation, canonical conjugate of δ

$\rho = 1/h$ Radius of curvature for a moving reference frame in a circular trajectory.

P_x, P_y, P_s: canonical momenta coordinates in a straight or curved reference frame. Note that for a circular trajectory: $v_s = (1+hx)\dot{s}$, $P_x = m\gamma\dot{x} + qA_x$, $P_y = m\gamma\dot{y} qA_y$ and $P_s = m\gamma\dot{s}(1+hx)^2 + q(1+hx)A_s$.

$p_x = P_x/P_0, p_y = P_x/P_0, p_s = P_s/P_0$ normalized momenta coordinates

$x' = P_x/P_s, y' = P_x/P_s$ transverse divergence coordinates

$x_p = P_x/P, y_p = P_y/P$ approximated divergence coordinates

$\delta = (P - P_0)/P_0$: normalized momentum deviation

$p_t = (E - E_0)/P_0 c$: normalized energy deviation

$p_\sigma = (E - E_0)/\beta_0 P_0 c$: SixTrack energy deviation canonical conjugate of σ

H Hamiltonian function

E_x, E_y, E_s Electric fields in a straight or curved reference frame

B_x, B_y, B_s Magnetic fluxes in a straight or curved reference frame

A_x, A_y, A_s Magnetic fluxes in a straight or curved reference frame

References

[1] F. Schmidt. SIXTRACK: Single particle tracking code treating transverse motion with synchrotron oscillations in a symplectic manner. Technical Report 94-56, CERN, 1994.

[2] A. Wrulich. RACETRACK: a computer code for the nonlinear particle motion in accelerators. Technical Report 84-026, DESY, 1984.

[3] G. Ripken. Non-linear canonical equations of coupled synchro-betatron motion and their solutions within the framework of a non-linear six-dimensional (symplectic) tracking program for ultrarelativistic protons. Technical Report 85-084, DESY, 1985.

[4] D.P. Barber, G. Ripken, and F. Schmidt. A non-linear canonical formalism for the coupled synchro-betatron motion of protons with arbitrary energy. Technical Report 87-36, DESY, 1987.

[5] G. Ripken and F. Schmidt. A symplectic six-dimensional thin-lens formalism for tracking. Technical Report DESY 95-63 and CERN/SL/95-12(AP), DESY, CERN, 1995.

[6] K. Heinemann, G. Ripken, and F. Schmidt. Construction of nonlinear symplectic six-dimensional thin-lens maps by exponentiation. Technical Report 95-189, DESY, 1995.

[7] D.P. Barber, K. Heinemann, G. Ripken, and F. Schmidt. Symplectic thin-lens transfer maps for SIXTRACK: Treatment of bending magnets in terms of the exact hamiltonian. Technical Report 96-156, DESY, 1996.

[8] L.H.A. Leunissen, F. Schmidt, and G. Ripken. 6D beam-beam kick including coupled motion. Technical report, 2001.

[9] A. Latina and R. De Maria. RF multipole implementation. Technical report, CERN-ATS. 2012-088.

[10] E. Forest. *Beam Dynamics: A New Attitude and Framework*. Harcourt Academic Publisher, 1999.

[11] A. Valishev and G. Stancari. Electron lens as beam-beam wire compensator in HL-LHC. 2013.

[12] F. Willeke and G. Ripken. Methods of beam optics. Technical Report 88-114, DESY, 1988.

[13] F. C. Iselin. The mad program (methodical accelerator design), physics methods manual. Technical Report CERN/SL/92-??, CERN, 1992.